

## Specific Aims

Many factors impact the successful management of the human airway during hospital procedures. These include, but are not limited to, technology availability, clinician competency, and natural and unnatural variations in the anatomy of a given patient. The general aim of this research is to develop a system that is not solely dependent on human manipulation, while still giving the physician full control of the procedure. Over the course of the 2021-2022 academic year, an Ohio State University capstone team has been developing a prototype that will achieve this aim (figure 3). The device utilizes an actuation method novel to the health-care community, twisted and coiled polymers (TCP), to guide the intubation tube into the proper location in the airway of the patient, before being extracted by the acting physician.

Current technology is limited primarily to direct and video laryngoscopes, as well as fiber optic intubation. These methods, while improving the visibility of the patient's anatomical features, require holistically manual control from the physician. This dependency leads to a large reliance on operator skill and judgment, giving way to increased chances for human error. There are multiple automated intubation systems currently in development, but none support the portability and automated extrusion that the prototype being discussed here can boast. By using the TCP actuation method, we are confident we can create a fully autonomous intubation method with the possibility for both manual and autonomous control, which also supports extrusion and retraction-based actuation.

The completed timeline for the project is shown in Figure 1, and is better explained in each of the individual Specific Aims sections.

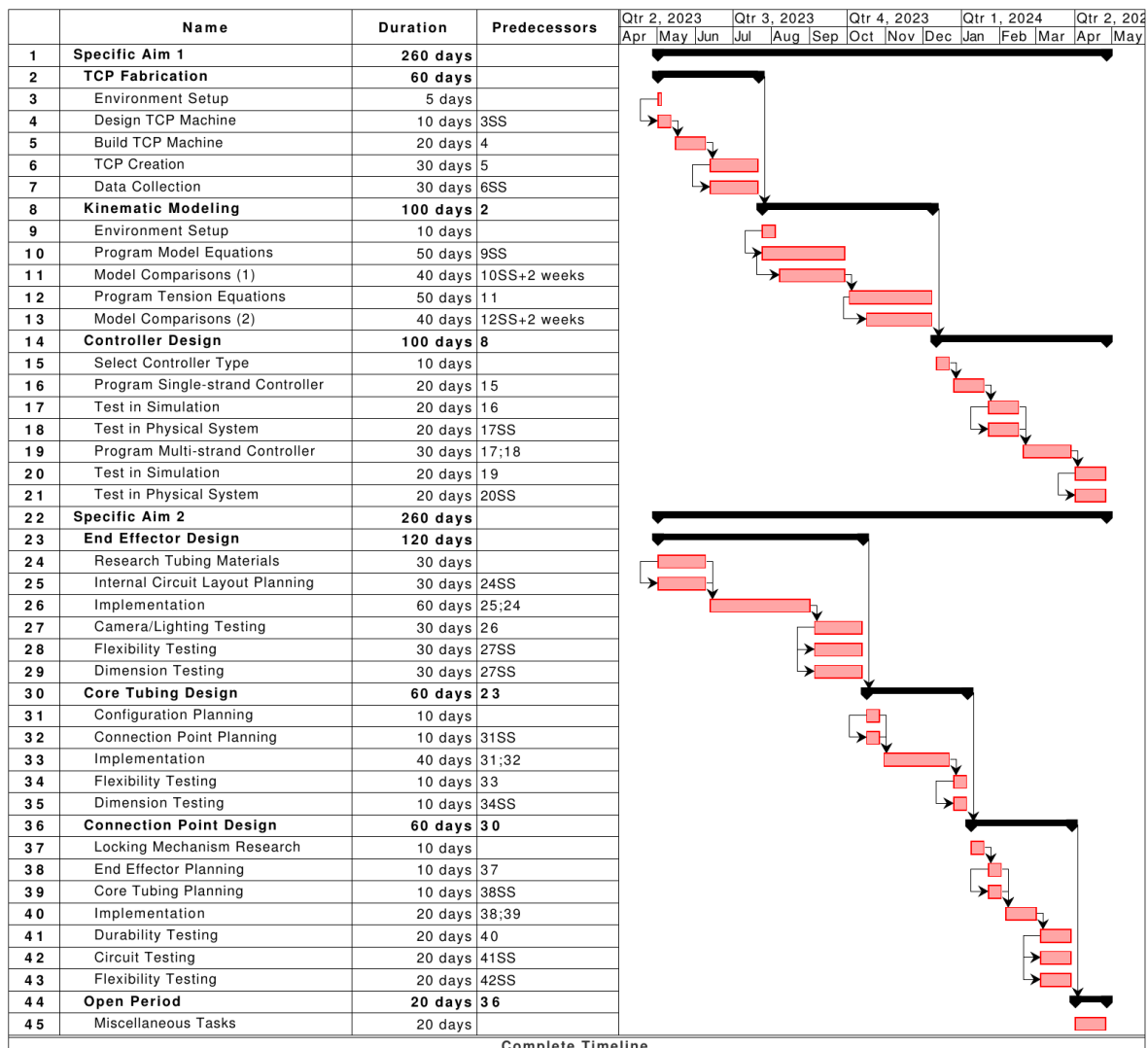


Figure 1: Full AEI Project Timeline

## **1 Aim 1: TCP Fabrication, Modeling, and Control**

Because of the unique properties of the actuation material, and for the purpose of data collection, the TCP material will be made in house. In the past, the material was created using a manually spun hand drill and imprecise counter-weight setup. With the intent of consistent recreation of the necessary string, the setup will be automated and configurable electronically. This step is very important to the overall performance of the project as consistency in the TCP material will be the difference between project success and project failure.

Once the desired fabrication setup is complete, the arguably most difficult portion of the design process will begin. Here, the researchers will build symbolic kinematic modeling equations such that the TCP end effector can be simulated and controlled using an optimal feedback controller. This will guarantee minimal error in intended versus actual movement. The system will be tested using inputs from a manual joystick controller, as well as with a predetermined path in order to simulate the inputs of the artificial intelligence system before it is officially ready for implementation (Aim 3).

## **2 Aim 2: Design of End Effector and Core Tubing**

In parallel to the modeling process, another objective is to design and implement the end effector and core tubing components. Since the end effector is objectively the highest risk component of the device, it will be designed to be completely removable from the rest of the core tubing. This will allow for easy replacement steps to be taken in the event of a broken end effector. With electrical connections set at designated positions, and held in place via a magnet and small locking mechanism. This is also where the camera at the end of the end effector (similar to the fiber optic camera) will be introduced and connected.

The remainder of the core tubing design is composed of an outer shell, electrical wiring to each of the four TCP, and electrical wiring to the camera. These components will be developed separately from the end effector with the exception of the connection point, and will be light weight, with the objective of minimizing the diameter of the final tube, this step is not seen as a primary obstacle. Note that the outer tubing of both portions of the continuum component must be compatible with the human anatomy.

## **3 Aim 3: Integration Between Neural Network and Controller**

In the fall of the 2021-2022 academic year the original capstone team, composed of mechanical and biomedical engineering students, and based out of the Biomedical Engineering Department, created a separate project for the creation of a neural network which can identify the human airway anatomy. The intent was to develop software which would eventually guide the continuum robot by identifying anatomical features in the mouth of a patient. This project was largely successful due to the cooperation of the Computer Science and Engineering (CSE) Department, and the software created is ready for implementation with a finished prototype.

Aim 3 of this project is to merge a final product with the artificial intelligence system created by the CSE team in the spring of 2022. This will consist of training a larger sample size of data, checking data conversions between the network and the main controller, and selecting a set of parameters which will be most useful in guiding the robot to the proper location.

## 4 Aim 1 Breakdown

### 4.1 Rationale

Aim 1 is centered around the creation and modeling of the TCP material. There are multiple methods used to make this process consistent and reliable. Most notably those described in [1], where the TCP actuation method is used to manipulate a humanoid hand. With the purpose of simplification of the creation/modeling process, a precursor fiber with similar specifications to that of the aforementioned article will be purchased.

In order to achieve a consistent fabrication process, the TCP will be spun using an automated system; similar to that of a rope making machine. The system will be configurable to a set number of rotations, and a set RPM speed, as well as having connections for an adjustable counter-weight which will be used as the third and final configuration input when making the material. Once the fabrication process is created and checked for consistency, data will be collected on the actuation capabilities of the string with varying configuration inputs. A setup will be chosen based on the data collected.

The next step is to derive a control model formula which can represent the tension exhibited by a single strand of the TCP with inputs of current [*Amps*] and over a predetermined length of time [*seconds*]. The constant parameters of the system will ideally be the same as the parameters used when creating the TCP string, but will require more testing to legitimize. Because TCP is actuated via heat generation, the system dynamics will be time-dependent, and will be discussed in the next section.

Finally, a controller will be implemented (figure 2), ideally using the aforementioned model formula. The current plan is to utilize an optimal control policy with the inclusion of an accurate model. In cases where the model cannot be applied, a simpler sub-optimal policy may be used instead. Both options are feasible. Model predictive control (MPC) will be considered because of its ability to look into future states, and accurately account for time-dependent variables when given a reliable and accurate model and cost function.

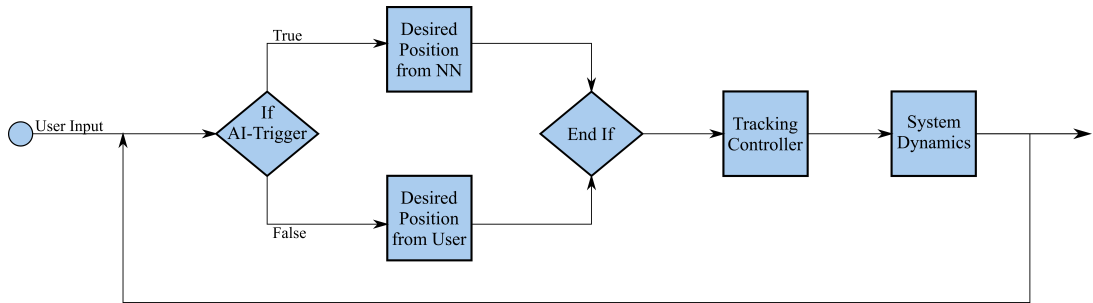


Figure 2: AEI System Control Diagram

Figure 2 shows the planned controller structure. The user-input block is a set of parameters received from the user during runtime. This will tell the device whether the user is in manual or automated operation modes, and will split into two similarly structured decision branches. With a desired trajectory chosen, the tracking controller will decide the necessary current value before uploading the results to the system dynamics and continuing.

### 4.2 Approach

#### 4.2.1 Timeline

The fabrication of the TCP material will be facilitated through a modular and controllable stepper motor circuit. The wire of choice will be silver-coated nylon 6/6 precursor fiber, similar to that used in the initial prototype. The control board used for TCP creation will be an Arduino Uno, and will be used to control the RPM of the machine, as well as the total number of spins. The counter-weight attached to the machine can also be adjusted for further variations, but will likely follow similar mechanics to those used in [1, 2, 3]. For consistency, the length of the TCP created during a given test will be held constant, and will be heat-treated and trained using the research verified by [1, 2]. The fabrication process is currently designated about 25% of total project time. That is, if the project spans a single year, the fabrication process would be given 3[months]. The bulk of this time period will be spent creating new material and collecting the data points outlined in Section 4.2.2.

Modeling of the TCP actuation will be completed in parallel to Aims 2 and 3, and will be appointed about 40% of the Aim 1 project schedule, meaning for a year-long project modeling will be given approximately

4.5[months]. The system of equations discussed in Section 4.2.2 from [1] make the assumption that the load place on the TCP is constant. For the purpose of implementation with the AEI system, this assumption cannot be made. The purpose of this portion of the project will be to implement a variable load into the system of equations, as well as merge the system with the continuum robot modeling techniques used in [4]. It should also be noted that some of this period will also be inevitably spent creating more TCP for the testing process.

The controller for the system will ideally be model-dependent. It is understood that model-dependent controllers, when accurately tuned, can create optimal systems and are more reliable and robust than model-independent alternatives. Considering the time-dependence of the TCP system variables, the use of model predictive control (MPC) will be considered because of its ability to look into future states and solve for the optimal set of inputs at a given point in time. MPC is a control method commonly used in the robotics community for like-wise scenarios and has proven to be one of the most ideal control policies in the field. That said, there are other similarly effective model-independent controller alternatives in the event that an optimal policy is not able to be constructed. Because of the importance of this portion of the project, it will similarly be allocated 40% of the total project time.

The completed timeline, as well as those constructed for Aim 2 and 3, are shown in Figure 1.

#### 4.2.2 Modeling Techniques

The following section describes the steps taken for TCP modeling as derived in *Modeling of twisted and coiled polymers (TCP) muscle based on phenomenological approach* by Farzad Karami and Yonas Tadesse. The following equations are used to approximate the temperature and displacement of the material based on a given current [ $A$ ], load [ $N$ ] and string dimensions.

The change in resistance with respect to temperature is shown in Equation 1 below.

$$R(T) = R_0(1 + \alpha(T - T_0)) \quad (1)$$

Where  $R(T)$  represents the current resistance in [ohms],  $R_0$  is the resistance at a reference temperature,  $T_0$ , and  $T$  is the current temperature of the TCP.  $\alpha$  is the coefficient of resistivity which is defined more accurately in [5] and is closely related to the coefficient of thermal expansion (CTE). For the purpose of manipulating tension using the TCP mechanics, a material with a negative CTE was chosen. It is further explored that the elastic modulus,  $E$ , is also determined by temperature.

For equation 1 to be used accurately during modeling the change in temperature must also be approximated. This is completed below.

$$T - T_\infty = -\frac{R_0 i^2}{-hA + R_0 i_2 \alpha} \left( 1 - \exp^{\frac{-hA + R_0 i_2 \alpha}{mc_p} t} \right) \quad (2)$$

Where  $T_\infty$  is the ambient temperature,  $i$  is the operating current,  $h$  is the coefficient of heat convection,  $A$  is the exposed TCP surface area,  $m$  is the TCP mass,  $c_p$  is the specific heat capacity, and  $t$  is the time-passed. This is used to approximate the temperature,  $T$ , of the TCP with respect to a given current,  $i$ , and time,  $t$ .

Using Equation 2 in combination with the function for  $E$  (equation 3 and along with the dimensions of the TCP material, the displacement of the TCP can be calculated using the set of equations shown below.

$$E(T) = a_1 T^{a_2} + a_3 \quad (3)$$

$$\Delta_{el} = \frac{F}{k} \quad (4)$$

$$\Delta_{th} = \delta H = \frac{L\delta L - \pi D \delta D}{\sqrt{L^2 - \pi D^2}} = \frac{L_0^2}{H_0} \alpha_L (T - T_0) - \frac{\pi i D_0^2}{H_0} \alpha_T (T - T_0) \quad (5)$$

$$\Delta H = H_0 - \Delta_{th} + \Delta_{el} \quad (6)$$

Equation 3 represents a fitted function for the elastic modulus of a single string of TCP at a given temperature. Equation 4 is the displacement of the TCP with respect to the load and equation 5 is the displacement based on the CTE and heat generation via electrical current. Finally, (6) is the sum of all displacement methods highlighted in the previous two equations.

Here,  $a_1$ ,  $a_2$  and  $a_3$  are the fitted curve coefficients,  $F$  is the load on the TCP,  $k$  is the elastic coefficient (not derived here),  $L_0$  is the initial TCP stretched length,  $H_0$  is the initial TCP coiled length,  $D_0$  is the

diameter of the coiled wire,  $\alpha_L$  is the longitudinal CTE, and  $\alpha_T$  is the transverse CTE. The use of these equations allow for the approximation of the TCP length at a given point in time.

The issue that arises here is the assumption that the load,  $F$ , is constant. For the purpose of implementation in AEI, the tension must be dynamic in the modeling. This issue will be addressed during the modeling

#### 4.2.3 Experimental Process

Verifying the controller system will be completed parallel to its programming. Once the fabrication method for the TCP is finalized, a few weeks will be designated to creating TCP and collecting data over its behavior when supplied with varying levels of current, constant counterweight magnitudes and with differing ply-numbers. The collected data points will include, but will not be limited to, TCP temperature, displacement and resistance trends.

With the load-static model verified, the system of equations will either be adjusted for variable load, or a method of numerically approximating the tension in the TCP will be implemented. The goal of this step will be to create a conversion from current TCP temperature to string tension. Modeling for tension will allow the researcher to design a single-strand controller which is capable of holding a desired displacement by manipulating the tension in the TCP wires.

With this, the system can be expanded to continuum robot modeling using the piecewise constant-curvature method, better explained in [4]. The controller can also be expanded to 3-D continuum robot actuation by similarly manipulating current to control deflection via the tension in the TCP.

At this step, the internal position sensing system will be addressed and there are multiple options available on the market. The intent with this component is to understand in real-time the position of the end effector, and compare to the model. These include electromagnetic sensing, explained thoroughly in [6], and optical sensing. Preliminary research suggests the former will be more viable for the purpose of the device and to the hospital environment.

### 4.3 Risks and Alternatives

It is understood that all of the steps taken in this portion of the development process are subject to considerable obstacles. That said, each of the discussed approaches have alternative methods of attack which should still achieve the overarching goals of the research.

In the case of fabrication, there are multiple methods for twisting, annealing, and training the TCP wires. This process is well documented in the aforementioned articles and is unlikely to be problematic, but if the creation process does not work as intended, there are many alternatives to twisting the string and prepping it for annealing and training. The TCP essentially requires a small-scale rope-making machine, and thus has many vehicles for a consistent system.

While methods of modeling the TCP behavior have been discussed, and are proven to be reliable, there is still a chance that a comprehensive model of the TCP will not be as easily generated as predicted. In the event that a model-based optimal controller cannot be constructed accurately, it is also possible to train a model-free neural network to produce the intended controller behavior. This would involve considerably more data on configuration details, but is very possible and has been done for likewise projects in the past [7, 8].

## 5 Aim 2 Breakdown

### 5.1 Rationale

In aim 2, the design of the end effector and core tubing circuitry is addressed. In this portion of the project, the end effector will be engineered to house the TCP such that it is not exposed, can be replaced when necessary, does not limit its range of motion, and also allows for the installment of the camera and light. To achieve this, the four strands of TCP will be lined in parallel to the center tube, which contains the necessary assortment of circuit components. It should be noted that this task is not dependent on the completion on Aim 1, as the TCP wires can be replicated with past test wire or thick string, and can be given a maximum TCP diameter which satisfies the constraint that the full prototype fits in the endotracheal tube.

The core tubing, which is extruded from the housing module and connects to the end effector via a specially designed clip, will likewise need to house the necessary wires which lead to the TCP, light and camera. This portion of the tubing will be relatively simple in configuration, with the primary limiting factor being the diameter of the tube.

Figure 3 shows the prototype designed and assembled by the aforementioned OSU capstone team. This prototype was specifically designed with the intent to prove functionality, and thus many quality-of-life

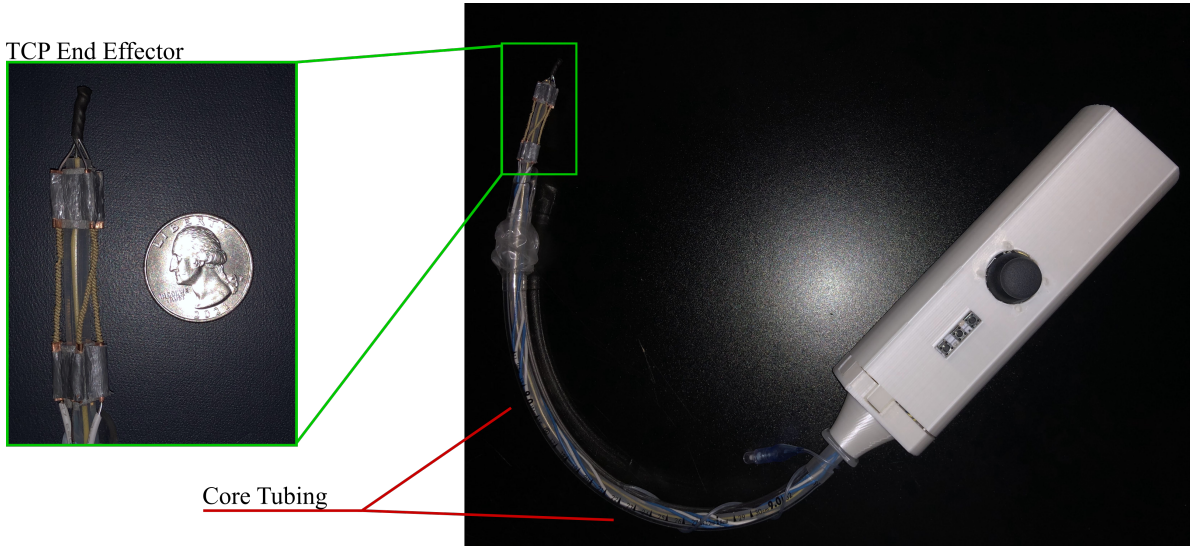


Figure 3: Prototype Assembly Developed in 2021-2022 Academic Year by OSU Capstone Team

features were not included. The most noticeable example of this being the exposed wiring at the prototype end effector, and the imprecise method of connection to the TCP ground wire. As this is the project being expanded upon, the previous prototype will be used as a reference for the general configuration of the tubing but will be largely redesigned.

## 5.2 Approach

### 5.2.1 Timeline

The timeline for the design and creation of the continuum snake will likely be more sequential than in Aim 1. Each of the components; the end effector, the core tubing and the connection between them, will be broken into itemized sections. More specifically, the end effector design segment, will most likely require close to 40% of the total project time. That is, for a year-long project, the end effector would be designated approximately 5[months]. This time is primarily split between researching airway-compatible flexible materials, and designing the internal layout for the TCP, camera and light configuration. It should be noted here that the circuit which controls the current to the individual TCP wires (without the camera/light) was created during the OSU capstone project, and will likely not be changed dramatically here. This circuit can be seen in Figure 4.

In the next segment, about 25% of project time will be appropriated to the design and creation of the core tubing (about 3[months] for a year-long project). This portion of the project is fundamentally simpler when compared to the first task, and is not seen as a large risk to project time. That said, the connection mechanism which allows for the smooth replacement of the end effector in the event of a breakage will be extremely important since the end effector is dependent on the wire connections and must be properly secured.

The design of the connection mechanism will occur after both the end effector and core tubing are completed, and is appointed 25% of the total project time (3[months] for a year-long project). This is because of the importance of this feature to the fast application necessary in the emergency environment. The remaining 10% of the project will be left open in the event that one or more of the sections requires slightly more time to be completed to the necessary standard.

The completed timeline, as well as those constructed for Aim 1 and 3, are shown in Figure 1.

### 5.2.2 Tubing/Circuitry Techniques

The end effector will be constructed with the intent of a two-layer configuration. The center will be comprised of the ground wire and the camera, similar to the prototype made during the OSU capstone project with an insulating tube surrounding the components (layer 1). Next, the TCP will be connected in parallel around the center shaft and connected to the common ground wire. Each string will also be connected to an individual active wire which is used to control the current supplied to the TCP from the main controller. The TCP will then be surrounded by another layer of insulated tubing (layer 2). It is also possible that

a third intermediate layer will be introduced to insulate the individual TCP string from one another, this will hopefully be avoidable though as it would unnecessarily increase the diameter of the assembled system. This portion of the device will only span one to two inches in length. Note that the controller need not be completed for testing, in initial scenarios, a simple user-defined analog signal can be used to test motion.

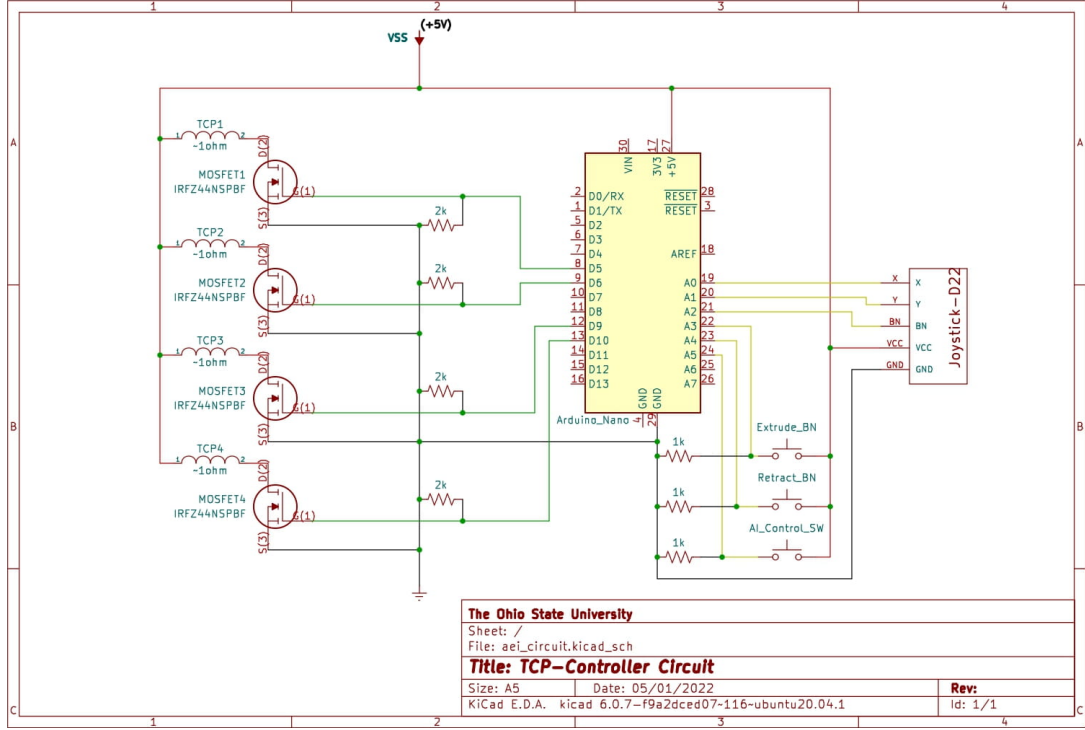


Figure 4: TCP Circuit Created in OSU Capstone Project

The TCP circuit is made up of three primary components; the four TCP strands and their designated MOSFET transistor which controls the variable current magnitude, the joystick which acts as a vehicle for manual operation of the end effector, and three buttons which control the extrusion, retraction, and AI features. The bulk of these items are housed in the control module (shown in Figure 3), leaving the TCP as the only remaining item which must be included in the end effector.

The core tubing will be considerably simpler to assemble and can be stylized to a single airway-compatible tube housing the necessary wires which will each be individually insulated. This is similar to every day USB pin-out wiring and other related cords. Because of its simplicity, the core tubing is not likely to break or have technical issues after being assembled. For this reason, the end effector and core tubing will be design separately and connected together via a locking mechanism. This way, if the end effector malfunctions, it can be replaced relatively easily, and without affecting the rest of the assembly. It may also be necessary to incorporate a aesthetic center-line down both components such that they can be attached to one another in a consistent configuration.

### 5.2.3 Experimental Process

The experimental process practiced here will primarily be focused on end-user compatibility, end effector flexibility, and dimension fitting. Since the prototype is obsolete if the end effector does not fit within the confines of the intubation tube, this specification will be prioritized. TCP string is known for its high degree of flexibility, one reason why it is ideal for working in such a tight environment [2]. That said, the inner components will most likely have to be optimized such that the dimension tests can be fulfilled reliably.

Flexibility tests will occur for the two main components separately, as well as for the final assembly. The prototype is currently planned to be slightly more rigid in the core tubing section than in the end effector. The end effector must be able to freely stretch in all directions in the full assembly. While the core tubing should be slightly more rigid, allowing it to be extruded from the control module reliably.

### **5.3 Risks and Alternatives**

The largest risk being addressed in this portion of development is the hard constraint for the diameter of the tubing. The most complex portion of the tubing, the end effector, must fit within the confines of commonly used intubating tubes. For development purposes, the constraint can be relaxed to the smallest adult-specific tube available (8[mm] diameter) instead of tubes used in children. That said, in the event that the TCP and other components do not fit within these constraints, alternatives to this configuration will have to be researched.

## References

- [1] Lianjun Wu et al. “Compact and low-cost humanoid hand powered by nylon artificial muscles”. In: *Bioinspir. Biomim.* 12.2 (Feb. 3, 2017), p. 026004. ISSN: 1748-3190. DOI: 10.1088/1748-3190/aa52f8. URL: <https://iopscience.iop.org/article/10.1088/1748-3190/aa52f8> (visited on 08/02/2022).
- [2] Carter S. Haines et al. “New twist on artificial muscles”. In: *Proceedings of the National Academy of Sciences* 113.42 (Oct. 18, 2016). Publisher: Proceedings of the National Academy of Sciences, pp. 11709–11716. DOI: 10.1073/pnas.1605273113. URL: <https://www.pnas.org/doi/full/10.1073/pnas.1605273113> (visited on 05/24/2022).
- [3] Lokesh Saharan and Yonas Tadesse. “Novel twisted and coiled polymer artificial muscles for biomedical and robotics applications”. In: *Materials for Biomedical Engineering*. Elsevier, 2019, pp. 45–75. ISBN: 978-0-12-816909-4. DOI: 10.1016/B978-0-12-816909-4.00003-8. URL: <https://linkinghub.elsevier.com/retrieve/pii/B9780128169094000038> (visited on 05/24/2022).
- [4] Priyanka Rao et al. “How to Model Tendon-Driven Continuum Robots and Benchmark Modelling Performance”. In: *Frontiers in Robotics and AI* 7 (2021). ISSN: 2296-9144. URL: <https://www.frontiersin.org/articles/10.3389/frobt.2020.630245> (visited on 07/27/2022).
- [5] Qianxi Yang and Guoqiang Li. “A top-down multi-scale modeling for actuation response of polymeric artificial muscles”. In: *Journal of the Mechanics and Physics of Solids* 92 (July 1, 2016), pp. 237–259. ISSN: 0022-5096. DOI: 10.1016/j.jmps.2016.04.007. URL: <https://www.sciencedirect.com/science/article/pii/S0022509615303537> (visited on 08/04/2022).
- [6] Hao Guo et al. “Continuum robot shape estimation using permanent magnets and magnetic sensors”. In: *Sensors and Actuators A: Physical* 285 (Jan. 2019), pp. 519–530. ISSN: 09244247. DOI: 10.1016/j.sna.2018.11.030. URL: <https://linkinghub.elsevier.com/retrieve/pii/S0924424718312974> (visited on 08/03/2022).
- [7] Simon X Yang and Max Meng. “An efficient neural network approach to dynamic robot motion planning”. In: *Neural Networks* 13.2 (Mar. 1, 2000), pp. 143–148. ISSN: 0893-6080. DOI: 10.1016/S0893-6080(99)00103-3. URL: <https://www.sciencedirect.com/science/article/pii/S0893608099001033> (visited on 06/22/2022).
- [8] Arunkumar Byravan and Dieter Fox. “SE3-nets: Learning rigid body motion using deep neural networks”. In: *2017 IEEE International Conference on Robotics and Automation (ICRA)*. 2017 IEEE International Conference on Robotics and Automation (ICRA). May 2017, pp. 173–180. DOI: 10.1109/ICRA.2017.7989023.
- [9] Michael Bernhard et al. “The First Shot Is Often the Best Shot: First-Pass Intubation Success in Emergency Airway Management”. In: *Anesthesia & Analgesia* 121.5 (Nov. 2015), pp. 1389–1393. ISSN: 0003-2999. DOI: 10.1213/ANE.0000000000000891. URL: <https://journals.lww.com/00000539-201511000-00039> (visited on 06/06/2022).
- [10] T. M. Hemmerling et al. “First robotic tracheal intubations in humans using the Kepler intubation system”. In: *British Journal of Anaesthesia* 108.6 (June 1, 2012). Publisher: Elsevier, pp. 1011–1016. ISSN: 0007-0912, 1471-6771. DOI: 10.1093/bja/aes034. URL: [https://www.bjanaesthesia.org/article/S0007-0912\(17\)32196-7/fulltext](https://www.bjanaesthesia.org/article/S0007-0912(17)32196-7/fulltext) (visited on 06/06/2022).
- [11] *Most Frequent Procedures Performed in U.S. Hospitals, 2011 - Statistical Brief #165*. URL: <https://www.hcup-us.ahrq.gov/reports/statbriefs/sb165.jsp> (visited on 06/06/2022).
- [12] Farzad Karami and Yonas Tadesse. “Modeling of twisted and coiled polymer (TCP) muscle based on phenomenological approach”. In: *Smart Mater. Struct.* 26.12 (Nov. 2017). Publisher: IOP Publishing, p. 125010. ISSN: 0964-1726. DOI: 10.1088/1361-665X/aa8d7d. URL: <https://doi.org/10.1088/1361-665X/aa8d7d> (visited on 06/22/2022).